

Singapore Management University

## Institutional Knowledge at Singapore Management University

---

Research Collection School Of Computing and Information Systems

School of Computing and Information Systems

---

11-1997

### Updated measurement of the $\tau$ lepton lifetime

R. BARATE

Manoj THULASIDAS

*Singapore Management University*, [manojt@smu.edu.sg](mailto:manojt@smu.edu.sg)

Follow this and additional works at: [https://ink.library.smu.edu.sg/sis\\_research](https://ink.library.smu.edu.sg/sis_research)



Part of the [Databases and Information Systems Commons](#)

---

#### Citation

1

This Journal Article is brought to you for free and open access by the School of Computing and Information Systems at Institutional Knowledge at Singapore Management University. It has been accepted for inclusion in Research Collection School Of Computing and Information Systems by an authorized administrator of Institutional Knowledge at Singapore Management University. For more information, please email [cherylds@smu.edu.sg](mailto:cherylds@smu.edu.sg).

# Updated measurement of the $\tau$ lepton lifetime

The ALEPH Collaboration<sup>‡</sup>

## Abstract

A new measurement of the mean lifetime of the  $\tau$  lepton is presented. Three different analysis methods are applied to a sample of 90000  $\tau$  pairs, collected in 1993 and 1994 with the ALEPH detector at LEP. The average of this measurement and those previously published by ALEPH is  $\tau_\tau = 290.1 \pm 1.5 \pm 1.1$  fs.

(To be published in Physics Letters B)

---

<sup>‡</sup>See the following pages for the list of authors.

# The ALEPH Collaboration

R. Barate, D. Buskulic, D. Decamp, P. Ghez, C. Goy, J.-P. Lees, A. Lucotte, M.-N. Minard, J.-Y. Nief, B. Pietrzyk

*Laboratoire de Physique des Particules (LAPP), IN<sup>2</sup>P<sup>3</sup>-CNRS, 74019 Annecy-le-Vieux Cedex, France*

M.P. Casado, M. Chmeissani, P. Comas, J.M. Crespo, M. Delfino, E. Fernandez, M. Fernandez-Bosman, Ll. Garrido,<sup>15</sup> A. Juste, M. Martinez, G. Merino, R. Miquel, Ll.M. Mir, C. Padilla, I.C. Park, A. Pascual, J.A. Perlas, I. Riu, F. Sanchez, F. Teubert

*Institut de Física d'Altes Energies, Universitat Autònoma de Barcelona, 08193 Bellaterra (Barcelona), Spain<sup>7</sup>*

A. Colaleo, D. Creanza, M. de Palma, G. Gelao, G. Iaselli, G. Maggi, M. Maggi, N. Marinelli, S. Nuzzo, A. Ranieri, G. Raso, F. Ruggieri, G. Selvaggi, L. Silvestris, P. Tempesta, A. Tricomi,<sup>3</sup> G. Zito

*Dipartimento di Fisica, INFN Sezione di Bari, 70126 Bari, Italy*

X. Huang, J. Lin, Q. Ouyang, T. Wang, Y. Xie, R. Xu, S. Xue, J. Zhang, L. Zhang, W. Zhao

*Institute of High-Energy Physics, Academia Sinica, Beijing, The People's Republic of China<sup>8</sup>*

D. Abbaneo, R. Alemany, U. Becker, A.O. Bazarko,<sup>20</sup> P. Bright-Thomas, M. Cattaneo, F. Cerutti, G. Dissertori, H. Drevermann, R.W. Forty, M. Frank, R. Hagelberg, J.B. Hansen, J. Harvey, P. Janot, B. Jost, E. Kneringer, J. Knobloch, I. Lehraus, P. Mato, A. Minten, L. Moneta, A. Pacheco, J.-F. Pustaszari,<sup>23</sup> F. Ranjard, G. Rizzo, L. Rolandi, D. Rousseau, D. Schlatter, M. Schmitt, O. Schneider, W. Tejessy, I.R. Tomalin, H. Wachsmuth, A. Wagner<sup>24</sup>

*European Laboratory for Particle Physics (CERN), 1211 Geneva 23, Switzerland*

Z. Ajaltouni, A. Barrès, C. Boyer, A. Falvard, C. Ferdi, P. Gay, C. Guicheney, P. Henrard, J. Jousset, B. Michel, S. Monteil, J.-C. Montret, D. Pallin, P. Perret, F. Podlyski, J. Proriot, P. Rosnet, J.-M. Rossignol

*Laboratoire de Physique Corpusculaire, Université Blaise Pascal, IN<sup>2</sup>P<sup>3</sup>-CNRS, Clermont-Ferrand, 63177 Aubière, France*

T. Fearnley, J.D. Hansen, J.R. Hansen, P.H. Hansen, B.S. Nilsson, B. Rensch, A. Wäänänen

*Niels Bohr Institute, 2100 Copenhagen, Denmark<sup>9</sup>*

G. Daskalakis, A. Kyriakis, C. Markou, E. Simopoulou, I. Siotis, A. Vayaki

*Nuclear Research Center Demokritos (NRCD), Athens, Greece*

A. Blondel, G. Bonneaud, J.C. Brient, P. Bourdon, A. Rougé, M. Rumpf, A. Valassi,<sup>6</sup> M. Verderi, H. Videau

*Laboratoire de Physique Nucléaire et des Hautes Energies, Ecole Polytechnique, IN<sup>2</sup>P<sup>3</sup>-CNRS, 91128 Palaiseau Cedex, France*

D.J. Candlin, M.I. Parsons

*Department of Physics, University of Edinburgh, Edinburgh EH9 3JZ, United Kingdom<sup>10</sup>*

E. Focardi, G. Parrini, K. Zachariadou

*Dipartimento di Fisica, Università di Firenze, INFN Sezione di Firenze, 50125 Firenze, Italy*

M. Corden, C. Georgiopoulos, D.E. Jaffe

*Supercomputer Computations Research Institute, Florida State University, Tallahassee, FL 32306-4052, USA<sup>13,14</sup>*

A. Antonelli, G. Bencivenni, G. Bologna,<sup>4</sup> F. Bossi, P. Campana, G. Capon, D. Casper, V. Chiarella, G. Felici, P. Laurelli, G. Mannocchi,<sup>5</sup> F. Murtas, G.P. Murtas, L. Passalacqua, M. Pepe-Altarelli

*Laboratori Nazionali dell'INFN (LNF-INFN), 00044 Frascati, Italy*

L. Curtis, S.J. Dorris, A.W. Halley, I.G. Knowles, J.G. Lynch, V. O'Shea, C. Raine, J.M. Scarr, K. Smith,

- P. Teixeira-Dias, A.S. Thompson, E. Thomson, F. Thomson, R.M. Turnbull  
*Department of Physics and Astronomy, University of Glasgow, Glasgow G12 8QQ, United Kingdom*<sup>10</sup>
- O. Buchmüller, S. Dhamotharan, C. Geweniger, G. Graefe, P. Hanke, G. Hansper, V. Hepp, E.E. Kluge, A. Putzer, J. Sommer, K. Tittel, S. Werner, M. Wunsch  
*Institut für Hochenergiephysik, Universität Heidelberg, 69120 Heidelberg, Fed. Rep. of Germany*<sup>16</sup>
- R. Beuselinck, D.M. Binnie, W. Cameron, P.J. Dornan, M. Girone, S. Goodsir, E.B. Martin, A. Moutoussi, J. Nash, J.K. Sedgbeer, P. Spagnolo, A.M. Stacey, M.D. Williams  
*Department of Physics, Imperial College, London SW7 2BZ, United Kingdom*<sup>10</sup>
- V.M. Ghete, P. Girtler, D. Kuhn, G. Rudolph  
*Institut für Experimentalphysik, Universität Innsbruck, 6020 Innsbruck, Austria*<sup>18</sup>
- A.P. Betteridge, C.K. Bowdery, P. Colrain, G. Crawford, A.J. Finch, F. Foster, G. Hughes, R.W.L. Jones, T. Sloan, M.I. Williams  
*Department of Physics, University of Lancaster, Lancaster LA1 4YB, United Kingdom*<sup>10</sup>
- A. Galla, I. Giehl, A.M. Greene, C. Hoffmann, K. Jakobs, K. Kleinknecht, G. Quast, B. Renk, E. Rohne, H.-G. Sander, P. van Gemmeren, C. Zeitnitz  
*Institut für Physik, Universität Mainz, 55099 Mainz, Fed. Rep. of Germany*<sup>16</sup>
- J.J. Aubert, C. Benchouk, A. Bonissent, G. Bujosa, J. Carr, P. Coyle, C. Diaconu, F. Etienne, N. Konstantinidis, O. Leroy, F. Motsch, P. Payre, M. Talby, A. Sadouki, M. Thulasidas, K. Trabelsi  
*Centre de Physique des Particules, Faculté des Sciences de Luminy, IN<sup>2</sup>P<sup>3</sup>-CNRS, 13288 Marseille, France*
- M. Aleppo, M. Antonelli, F. Ragusa<sup>2</sup>  
*Dipartimento di Fisica, Università di Milano e INFN Sezione di Milano, 20133 Milano, Italy*
- R. Berlich, W. Blum, V. Büscher, H. Dietl, G. Ganis, C. Gotzhein, H. Kroha, G. Lütjens, G. Lutz, W. Männer, H.-G. Moser, R. Richter, A. Rosado-Schlosser, S. Schael, R. Settles, H. Seywerd, R. St. Denis, H. Stenzel, W. Wiedenmann, G. Wolf  
*Max-Planck-Institut für Physik, Werner-Heisenberg-Institut, 80805 München, Fed. Rep. of Germany*<sup>16</sup>
- J. Boucrot, O. Callot,<sup>2</sup> S. Chen, Y. Choi,<sup>21</sup> A. Cordier, M. Davier, L. Duflot, J.-F. Grivaz, Ph. Heusse, A. Höcker, A. Jacholkowska, M. Jacquet, D.W. Kim,<sup>12</sup> F. Le Diberder, J. Lefrançois, A.-M. Lutz, I. Nikolic, M.-H. Schune, S. Simion, E. Tournefier, J.-J. Veillet, I. Videau, D. Zerwas  
*Laboratoire de l'Accélérateur Linéaire, Université de Paris-Sud, IN<sup>2</sup>P<sup>3</sup>-CNRS, 91405 Orsay Cedex, France*
- P. Azzurri, G. Bagliesi, G. Batignani, S. Bettarini, C. Bozzi, G. Calderini, M. Carpinelli, M.A. Ciocci, V. Ciulli, R. Dell'Orso, R. Fantechi, I. Ferrante, L. Foà,<sup>1</sup> F. Forti, A. Giassi, M.A. Giorgi, A. Gregorio, F. Ligabue, A. Lusiani, P.S. Marrocchesi, A. Messineo, F. Palla, G. Sanguinetti, A. Sciabà, J. Steinberger, R. Tenchini, G. Tonelli,<sup>19</sup> C. Vannini, A. Venturi, P.G. Verdini  
*Dipartimento di Fisica dell'Università, INFN Sezione di Pisa, e Scuola Normale Superiore, 56010 Pisa, Italy*
- G.A. Blair, L.M. Bryant, J.T. Chambers, Y. Gao, M.G. Green, T. Medcalf, P. Perrodo, J.A. Strong, J.H. von Wimmersperg-Toeller  
*Department of Physics, Royal Holloway & Bedford New College, University of London, Surrey TW20 OEX, United Kingdom*<sup>10</sup>
- D.R. Botterill, R.W. Clift, T.R. Edgecock, S. Haywood, P.R. Norton, J.C. Thompson, A.E. Wright  
*Particle Physics Dept., Rutherford Appleton Laboratory, Chilton, Didcot, Oxon OX11 0QX, United Kingdom*<sup>10</sup>
- B. Bloch-Devaux, P. Colas, S. Emery, W. Kozanecki, E. Lançon, M.C. Lemaire, E. Locci, P. Perez, J. Rander, J.-F. Renardy, A. Roussarie, J.-P. Schuller, J. Schwindling, A. Trabelsi, B. Vallage  
*CEA, DAPNIA/Service de Physique des Particules, CE-Saclay, 91191 Gif-sur-Yvette Cedex, France*<sup>17</sup>

S.N. Black, J.H. Dann, R.P. Johnson, H.Y. Kim, A.M. Litke, M.A. McNeil, G. Taylor

*Institute for Particle Physics, University of California at Santa Cruz, Santa Cruz, CA 95064, USA<sup>22</sup>*

C.N. Booth, R. Boswell, C.A.J. Brew, S. Cartwright, F. Combley, M.S. Kelly, M. Lehto, W.M. Newton, J. Reeve, L.F. Thompson

*Department of Physics, University of Sheffield, Sheffield S3 7RH, United Kingdom<sup>10</sup>*

A. Böhrer, S. Brandt, G. Cowan, C. Grupen, G. Lutters, P. Saraiva, L. Smolik, F. Stephan

*Fachbereich Physik, Universität Siegen, 57068 Siegen, Fed. Rep. of Germany<sup>16</sup>*

M. Apollonio, L. Bosisio, R. Della Marina, G. Giannini, B. Gobbo, G. Musolino

*Dipartimento di Fisica, Università di Trieste e INFN Sezione di Trieste, 34127 Trieste, Italy*

J. Putz, J. Rothberg, S. Wasserbaech

*Experimental Elementary Particle Physics, University of Washington, WA 98195 Seattle, U.S.A.*

S.R. Armstrong, E. Charles, P. Elmer, D.P.S. Ferguson, S. González, T.C. Greening, O.J. Hayes, H. Hu, S. Jin, P.A. McNamara III, J.M. Nachtman, J. Nielsen, W. Orejudos, Y.B. Pan, Y. Saadi, I.J. Scott, J. Walsh, Sau Lan Wu, X. Wu, J.M. Yamartino, G. Zoebnig

*Department of Physics, University of Wisconsin, Madison, WI 53706, USA<sup>11</sup>*

---

<sup>1</sup>Now at CERN, 1211 Geneva 23, Switzerland.

<sup>2</sup>Also at CERN, 1211 Geneva 23, Switzerland.

<sup>3</sup>Also at Dipartimento di Fisica, INFN, Sezione di Catania, Catania, Italy.

<sup>4</sup>Also Istituto di Fisica Generale, Università di Torino, Torino, Italy.

<sup>5</sup>Also Istituto di Cosmo-Geofisica del C.N.R., Torino, Italy.

<sup>6</sup>Supported by the Commission of the European Communities, contract ERBCHBICT941234.

<sup>7</sup>Supported by CICYT, Spain.

<sup>8</sup>Supported by the National Science Foundation of China.

<sup>9</sup>Supported by the Danish Natural Science Research Council.

<sup>10</sup>Supported by the UK Particle Physics and Astronomy Research Council.

<sup>11</sup>Supported by the US Department of Energy, grant DE-FG0295-ER40896.

<sup>12</sup>Permanent address: Kangnung National University, Kangnung, Korea.

<sup>13</sup>Supported by the US Department of Energy, contract DE-FG05-92ER40742.

<sup>14</sup>Supported by the US Department of Energy, contract DE-FC05-85ER250000.

<sup>15</sup>Permanent address: Universitat de Barcelona, 08208 Barcelona, Spain.

<sup>16</sup>Supported by the Bundesministerium für Bildung, Wissenschaft, Forschung und Technologie, Fed. Rep. of Germany.

<sup>17</sup>Supported by the Direction des Sciences de la Matière, C.E.A.

<sup>18</sup>Supported by Fonds zur Förderung der wissenschaftlichen Forschung, Austria.

<sup>19</sup>Also at Istituto di Matematica e Fisica, Università di Sassari, Sassari, Italy.

<sup>20</sup>Now at Princeton University, Princeton, NJ 08544, U.S.A.

<sup>21</sup>Permanent address: Sung Kyun Kwan University, Suwon, Korea.

<sup>22</sup>Supported by the US Department of Energy, grant DE-FG03-92ER40689.

<sup>23</sup>Now at School of Operations Research and Industrial Engineering, Cornell University, Ithaca, NY 14853-3801, U.S.A.

<sup>24</sup>Now at Schweizerischer Bankverein, Basel, Switzerland.

# 1 Introduction

In the Standard Model, the weak charged-current coupling strength is assumed to be the same for all fermion doublets. This hypothesis may be tested in the lepton sector by comparing the rates of certain decays. The most precise universality tests involving the  $\tau$ - $\nu_\tau$  doublet are presently obtained from measurements of the decays  $\tau^- \rightarrow e^- \nu \bar{\nu}$ ,  $\tau^- \rightarrow \mu^- \nu \bar{\nu}$ , and  $\mu^- \rightarrow e^- \nu \bar{\nu}$ , the sensitivity being limited by the experimental uncertainties on the  $\tau$  lifetime and branching fractions.

Presented in this paper is an updated measurement of the  $\tau$  lifetime, based on the momentum-dependent impact parameter sum (MIPS) method, the impact parameter difference (IPD) method, and the decay length (DL) method. The MIPS and IPD analyses are applied to the  $e^+e^- \rightarrow \tau^+\tau^-$  events in which each  $\tau$  decays to a final state containing a single charged track (“1-1 topology”). The MIPS measurement has a small statistical uncertainty because the impact parameter smearing related to the size of the luminous region is nearly canceled in the sum of the impact parameters of the two daughter tracks. The result is, however, sensitive to the assumed impact parameter resolution. On the other hand, the IPD measurement is subject to a statistical error from the size of the luminous region but is insensitive to the assumed resolution. The DL method yields a precise lifetime measurement from  $\tau$ ’s decaying into three-prong final states. The dominant source of uncertainty is the statistical uncertainty related to the natural width of the exponential lifetime distribution; the size of the luminous region yields a negligible contribution to the lifetime uncertainty. Brief descriptions of the MIPS, IPD, and DL methods are given below; more details are available in [1–3]. The ALEPH measurement of the  $\tau$  lifetime is further supplemented by an analysis [4] based on the three-dimensional impact parameter sum (3DIP) method. The 3DIP method relies on kinematic constraints to reduce the  $\tau$  direction uncertainty in events containing two hadronic  $\tau$  decays.

The data were collected at the LEP  $e^+e^-$  collider, at centre of mass energies around the Z resonance. A  $\tau$  mass of  $m_\tau = 1777.00^{+0.30}_{-0.27}$  MeV/ $c^2$  [5] is assumed throughout this paper.

## 2 Apparatus and data sample

The ALEPH detector is described in detail in [6,7]. The tracking system consists of a high-resolution silicon strip vertex detector (VDET), a cylindrical drift chamber (the inner tracking chamber or ITC), and a large time projection chamber (TPC). The VDET comprises two layers of double-sided silicon strip detectors at average radii of 6.3 and 10.8 cm. The spatial resolution for  $r$ - $\phi$  coordinates is  $12 \mu\text{m}$  and varies between 12 and  $22 \mu\text{m}$  for  $z$  coordinates, depending on track polar angle. The angular coverage is  $|\cos\theta| < 0.85$  for the inner layer and  $|\cos\theta| < 0.69$  for the outer layer. The ITC has eight coaxial wire layers at radii from 16 to 26 cm. The TPC provides up to 21 three-dimensional coordinates per track at radii between 40 and 171 cm. The tracking detectors are contained within a superconducting solenoid, which produces an axial magnetic field of 1.5 T. Charged tracks measured in the VDET-ITC-TPC system are reconstructed with a momentum resolution of  $\Delta p/p = 6 \times 10^{-4} p_t \oplus 0.005$  ( $p_t$  in GeV/ $c$ ). An impact parameter resolution of  $28 \mu\text{m}$  in the  $r$ - $\phi$  plane is achieved for muons from  $Z \rightarrow \mu^+\mu^-$  having at least

one VDET  $r$ - $\phi$  hit.

Surrounding the TPC is an electromagnetic calorimeter (ECAL), a lead/wire-chamber sandwich operated in proportional mode. The calorimeter is read out via projective towers subtending typically  $0.9^\circ \times 0.9^\circ$  in solid angle which sum the deposited energy in three sections in depth. Beyond the ECAL lies the solenoid, followed by a hadron calorimeter (HCAL), which uses the iron return yoke as absorber and has an average depth of 1.50 m. Hadronic showers are sampled by 23 planes of streamer tubes, providing a digital hit pattern and inducing an analog signal on pads arranged in projective towers. The HCAL is used in combination with two layers of muon chambers outside the magnet for  $\mu$  identification.

The analysis is based on data samples collected in 1993 and 1994, corresponding to an estimated 31900 and 82700 produced  $\tau$  pairs, respectively. The combined sample of  $e^+e^- \rightarrow \tau^+\tau^-$  events consists of 3.5% collected at  $\sqrt{s} = 89.4$  GeV, 91.4% at 91.2 GeV (Z “peak”), and 5.1% at 93.0 GeV. All of the off-peak data were obtained in 1993. The data from the two years are analyzed separately. No inconsistencies between the samples are observed. The results presented herein refer to the combination of the two data sets.

Tau-pair candidate events are selected by means of an improved version of the algorithm described in [8]. The modifications make the selection less sensitive to low-energy clusters in the calorimeters. The overall efficiency of this algorithm is 78%, with an expected background contamination of 1.3% at the Z peak. A total of 90408 candidate  $\tau^+\tau^-$  events are selected. Further selection criteria are then imposed to isolate well-reconstructed one-prong and three-prong  $\tau$  decays for the different lifetime analyses.

Monte Carlo  $\tau^+\tau^-$  events [9] are used to study biases in the analysis methods. An independent sample is generated for each year of data taking to simulate the applicable detector conditions, beam sizes, and centre of mass energies. The input  $\tau$  lifetime is 296 fs. Background events from  $e^+e^- \rightarrow e^+e^-$  [10],  $e^+e^- \rightarrow \mu^+\mu^-$  [9],  $e^+e^- \rightarrow q\bar{q}$  [11], and two-photon interactions [12] are also simulated.

In the following,  $d$  denotes the impact parameter of a reconstructed daughter track, measured in the  $r$ - $\phi$  plane with respect to the nominal interaction point. The sign of  $d$  is defined to be that of the  $z$  component of the particle’s angular momentum about this point.

Reconstructed track impact parameters are corrected for systematic offsets in both  $d$  and  $z$  due to detector alignment and drift field parametrization errors. The offsets are measured as a function of  $\theta$  and  $\phi$  from  $Z \rightarrow q\bar{q}$  events. The corrections have an rms of  $14 \mu\text{m}$  in  $d$  and  $20 \mu\text{m}$  in  $z$ . Similar results are obtained from  $Z \rightarrow \mu^+\mu^-$  events, confirming that the offsets do not depend appreciably on track momentum. These corrections have a small effect and are taken into account in the evaluation of the systematic uncertainty in each analysis.

The beam axis position in the  $xy$  plane is determined from selected reconstructed charged tracks in Z decay events (excluding  $\tau$  pairs), averaged over blocks of roughly 75 consecutive events. The typical uncertainties are  $20 \mu\text{m}$  in  $x$  (horizontally) and  $10 \mu\text{m}$  in  $y$  (vertically). The size of the luminous region along  $x$  (typically  $159 \mu\text{m}$  rms in 1993 and  $125 \mu\text{m}$  in 1994, due to different LEP optics) is measured from the fitted primary vertices of selected  $Z \rightarrow q\bar{q}$  events, over blocks of about 270 events. The size in the  $y$  direction is taken to be  $5 \mu\text{m}$  rms. The measured  $z$  dimensions, 7.4 mm in 1993 and 7.0 mm in 1994,

are used in the DL analysis.

### 3 Momentum-dependent impact parameter sum analysis

The MIPS method [3] is applied to  $\tau^+\tau^-$  events of 1-1 topology. The mean  $\tau$  lifetime is measured by means of a maximum likelihood fit to the distribution of the impact parameter sum  $\delta = d_+ + d_-$ , where  $d_+$  and  $d_-$  denote the impact parameters of the two charged daughter tracks. The mean lifetime determines the overall scale of the true  $\delta$  distribution; typical  $\delta$  values are on the order of  $c\tau_\tau \simeq 88 \mu\text{m}$ . The likelihood function is constructed to take into account, on an event-by-event basis, the dependence of the  $\delta$  distribution on the momenta  $p_\pm$  of the daughters. A large sample of Monte Carlo events is used to parametrize this dependence for each event helicity combination,  $\tau_L^- \tau_R^+$  and  $\tau_R^- \tau_L^+$ . The likelihood function for each event includes contributions from both event helicities according to the measured  $\tau$  polarization [13] as a function of the  $\tau^-$  polar angle and  $\sqrt{s}$ .

The fitted lifetime is sensitive to the  $d$  resolution assumed in the likelihood function. The  $d$  resolution function for each daughter track is taken to be the sum of three Gaussian functions whose widths and amplitudes are parametrized [3] in terms of momentum, polar angle, and the  $d$  uncertainty calculated by the track fitting program. The parameters of the resolution core and near tails are obtained from studies of  $e^+e^- \rightarrow e^+e^-$ ,  $e^+e^- \rightarrow \mu^+\mu^-$ ,  $\gamma\gamma \rightarrow e^+e^-$ , and  $\gamma\gamma \rightarrow \mu^+\mu^-$  events in the data. The parameters of the far tails, dominated by photon conversions (which can cause pattern recognition errors) and nuclear interactions in hadronic  $\tau$  decays, are extracted from a sample of simulated  $\tau^+\tau^-$  events. The rms of the core is typically 25 to 100  $\mu\text{m}$ . The second (third) Gaussian function contains roughly 5% (0.2%) of the tracks and is 3.3 ( $\sim 20$ ) times wider than the core. Finally, the small smearing in  $\delta$  related to the size of the luminous region (typically 5  $\mu\text{m}$  rms) is taken into account in the likelihood function.

The event selection [3] yields 40271 candidate events. A few remaining events with poorly measured tracks are removed by means of a cut on the event confidence level (CL). The CL of an event is defined to be the integrated probability density for the event to have a reconstructed  $|\delta|$  equal to or larger than the observed value; a mean  $\tau$  lifetime of 293.7 fs [3] is assumed in this calculation. The requirement  $\text{CL} > 0.01\%$  removes 29 events from the sample. The fits to the data yield an (uncorrected) mean  $\tau$  lifetime of  $289.1 \pm 1.8$  fs. Figure 1 shows the  $\delta$  distribution for the data.

The same procedure, including the parametrization of the  $d$  resolution, is followed with Monte Carlo  $e^+e^- \rightarrow \ell^+\ell^-$  and  $\gamma\gamma \rightarrow \ell^+\ell^-$  events ( $\ell = e, \mu, \tau$ ) generated at  $\sqrt{s} = 91.25$  GeV. The different dimensions of the luminous region in 1993 and 1994 are taken into account in the fits to the Monte Carlo events. The possible lifetime bias in the method is determined from a comparison of the fitted lifetime with the generated value; the resulting bias is  $(+0.24 \pm 0.63)\%$ , where the uncertainty is from Monte Carlo statistics. The systematic error associated with the use of peak Monte Carlo events to simulate off-peak data is negligible.

The calculated biases are used to correct the results of the fits to the data; the Monte Carlo fit uncertainty is therefore treated as a systematic uncertainty on the measured



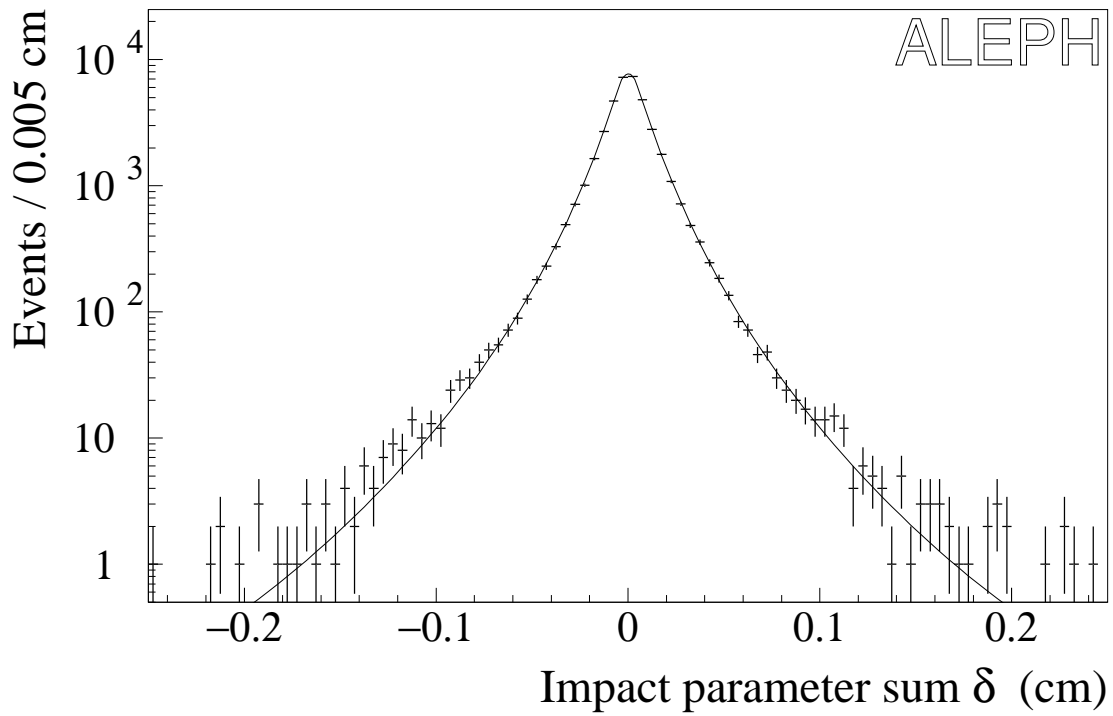


Figure 1: Impact parameter sum distribution for 1993 and 1994 data. The curve represents the sum of the functions obtained from separate fits to the two data samples.

Table 1: Systematic biases and uncertainties in the MIPS analysis.

Source	Bias and uncertainty (%)
$\tau^+\tau^-$ Monte Carlo bias	$+0.24 \pm 0.63$
$d$ resolution parametrization	$\pm 0.95$
Variation of CL cut	$\pm 0.25$
Transverse $\tau$ polarization correlation	$+0.22 \pm 0.22$
Branching fractions	$-0.06 \pm 0.13$
Backgrounds	$-0.36 \pm 0.09$
Total	$+0.04 \pm 1.20$

lifetime. The systematic biases and uncertainties are summarized in Table 1.

The systematic uncertainty associated with the  $d$  resolution parametrization includes contributions from (1) the limitations of the resolution model, estimated from a comparison of the parameters derived from simulated  $\tau^+\tau^-$  vs.  $e^+e^-$  and  $\mu^+\mu^-$  events; (2) the statistical uncertainty on the parameters measured from real  $e^+e^-$  and  $\mu^+\mu^-$  events; (3) the statistical uncertainty on the parameters of the far tails, measured from simulated  $\tau^+\tau^-$  events; and (4) the simulation accuracy of the far tail parameters, estimated from a comparison of real and simulated  $e^+e^-$ ,  $\mu^+\mu^-$ , and  $q\bar{q}$  events. An additional test of the resolution in the  $\tau^+\tau^-$  sample is performed in which the CL cut value is varied between 0 and 0.5%. The resulting variations of the fitted lifetime in data and Monte Carlo agree within the expected statistical fluctuations; the assigned systematic uncertainty, 0.25%, reflects the sensitivity of the test. Any remaining detector alignment errors are implicitly taken into account in the  $d$  resolution parametrization.

The correlation of the transverse polarizations of the  $\tau^+$  and  $\tau^-$  is not simulated in the event generator [9] used for the final lifetime bias determination, so a special generator [14] without initial or final state radiation is used to determine the effective bias due to this correlation,  $(+0.22 \pm 0.22)\%$ . The uncertainty associated with the longitudinal  $\tau$  polarization is negligible.

Each  $\tau$  decay mode produces a different impact parameter distribution. The differences between the measured  $\tau$  branching fractions [15,16] and those used in the Monte Carlo simulation are expected to yield a bias of  $-0.06\%$  on the measured lifetime. The uncertainties on the measured branching fractions correspond to a lifetime uncertainty of 0.13%.

The bias due to background events is predicted from Monte Carlo simulation to be  $(-0.36 \pm 0.09)\%$ , where the uncertainty includes a systematic contribution of 25%, estimated from a comparison of the real and simulated distributions of the discriminating variables used in the  $\tau^+\tau^-$  event selection. The reaction  $\gamma\gamma \rightarrow \ell^+\ell^-$  is the dominant source of contamination in the 1-1 sample, amounting to 0.27%. The contamination from cosmic rays is measured to be less than 0.01%.

The net systematic bias is  $(+0.04 \pm 1.20)\%$ . The  $\tau$  lifetime result, corrected for biases, is

$$\tau_\tau = 289.0 \pm 1.8 \text{ (stat)} \pm 3.5 \text{ (syst) fs.} \quad (1)$$

## 4 Impact parameter difference analysis

The 1-1 topology events are also analyzed with the IPD method [1]. In this method the following quantities are determined for each event:

$$\begin{aligned} Y &= d_+ - d_- , \\ X &= \frac{\bar{p}_\tau(\sqrt{s})}{\bar{p}_\tau^0} \Delta\phi \sin \theta , \end{aligned} \quad (2)$$

where  $\bar{p}_\tau(\sqrt{s})$  is the mean  $\tau$  momentum, determined from Monte Carlo simulation after all event selection criteria are applied,  $\bar{p}_\tau^0 = 45.40 \text{ GeV}/c$  is the mean  $\tau$  momentum at  $\sqrt{s} = 91.25 \text{ GeV}$ ,  $\Delta\phi = \phi_+ - \phi_- \pm \pi$  is the acoplanarity of the two daughter tracks, and  $\theta$  is taken to be the polar angle of the event thrust axis, calculated from the reconstructed charged and neutral particles. No estimate of the  $\tau$  direction is needed to determine  $\Delta\phi$ . For a given value of  $X$ , the expected value of  $Y$  is given by [1]

$$\langle Y \rangle = \left[ \frac{\bar{p}_\tau^0}{m_\tau} \tau_\tau \right] X , \quad (3)$$

i.e., the slope of  $\langle Y \rangle$  vs.  $X$  is equal to the mean  $\tau$  decay length in the laboratory frame. This relation holds in the approximation that the  $\tau^+$  and  $\tau^-$  are back to back in the  $r$ - $\phi$  projection and the  $\tau$  decay angles are small in the lab.

Equation 3 is not satisfied for radiative  $Z \rightarrow \tau^+\tau^-$  events; such events are rejected by a cut on the invariant mass of the charged daughter and the photon candidates in each event hemisphere. The parameters of the line  $\langle Y \rangle = a_0 + a_1 X$  are then extracted by means of an unbinned least-squares fit, and the mean  $\tau$  lifetime is computed from the fitted slope  $a_1$ . Event  $i$  is weighted by  $1/(\Delta Y_i)^2$  in the fit, where  $\Delta Y_i$ , the expected rms smearing on  $Y_i$ , includes contributions from the estimated tracking resolution for event  $i$ , the size of the luminous region (a function of  $\phi_\pm$ ), and the natural spread of  $Y_i$  (a function of  $X_i$ ). The fit range  $|X| < 0.18$  is chosen in order to reduce the effect of mismeasured tracks, radiative events, and background from two-photon interactions; 38120 events enter the fit. An iterative trimming procedure is used to remove events with fit residuals in  $Y$  greater in magnitude than  $\Delta_{trim} = 0.137 \text{ cm}$ , most of which contain mismeasured tracks. This procedure removes 78 events.

The fits to the data yield  $a_1 = +0.2218 \pm 0.0023 \text{ cm}$  and  $a_0 = +0.0004 \pm 0.0001 \text{ cm}$  (Fig. 2); the  $\chi^2$  per degree of freedom is 1.02, implying that  $\Delta Y_i$  is correctly parametrized. The small positive offset in  $a_0$  is caused by bremsstrahlung and other track measurement errors and agrees with the value predicted from Monte Carlo events.

Simulated events are used to study and correct for the bias in the determination of the mean  $\tau$  decay length from the  $Y$  vs.  $X$  distribution. The dependence of  $a_1$  on  $\tau_\tau$  is influenced by the following effects: (1) The selection procedure may introduce a bias on the lifetime. (2) Surviving radiative events violate the assumption that the  $\tau^+$  and  $\tau^-$  are back to back; they also cause the mean  $\tau$  momentum to depend slightly on  $|X|$ . (3) There is a bias associated with the approximation that the  $\tau$  decay angles are small in the lab system. (4) Tracking errors on  $d$  and  $\phi$  introduce a positive bias on  $a_1$ , which is reduced by the trimming in the fit. (5) Background events affect the fitted slope. These biases and all systematic uncertainties are given in Table 2. The net bias is  $(-0.29 \pm 0.20)\%$ , where the uncertainty is from Monte Carlo statistics.

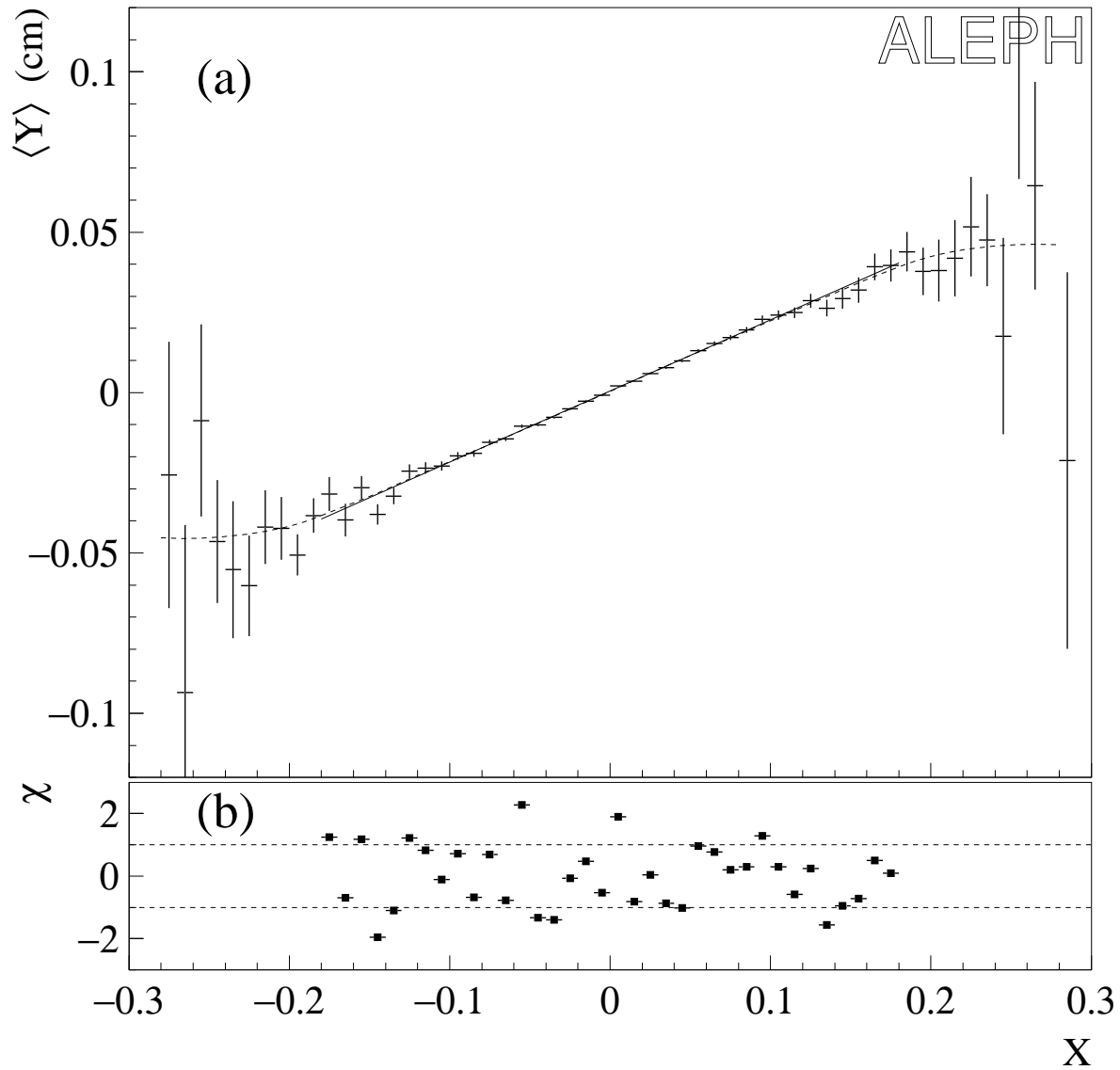


Figure 2: (a)  $\langle Y \rangle$  vs.  $X$  for the 1993 and 1994 data. The solid line represents the fit results. The dashed curve shows the shape of  $\langle Y \rangle$  vs.  $X$  for simulated  $\tau^+\tau^-$  and background events. (b) Plot of pulls (deviation from fitted line divided by uncertainty).

Table 2: Systematic biases and uncertainties in the IPD analysis. The first uncertainty is from Monte Carlo statistics and the second is systematic.

Source	Bias and uncertainty (%)
Selection bias	$-0.02 \pm 0.11$
Radiative events	$-0.47 \pm 0.03 \pm 0.09$
Small decay angle approximation	$-0.12 \pm 0.01$
Tracking resolution and trimming	$+0.54 \pm 0.16 \pm 0.35$
Backgrounds	$-0.22 \pm 0.04 \pm 0.06$
Detector alignment	$\pm 0.15$
Total	$-0.29 \pm 0.20 \pm 0.40$

In addition to the statistical errors from the Monte Carlo simulation, the following systematic errors are considered. The simulation of final state radiation in selected  $Z \rightarrow \tau^+\tau^-$  decays, relevant to Bias 2 above, is verified in an analysis of isolated photons in data and Monte Carlo. The lifetime uncertainty associated with the simulation of the tracking resolution, including multiple scattering, bremsstrahlung, and nuclear interactions, is evaluated from studies of the  $\tau^+\tau^-$  events as well as Bhabha, dimuon, and two-photon events in data and Monte Carlo. A systematic uncertainty of 25% is assigned on the bias from each background source. The uncertainty associated with detector alignment errors is taken to be half the effect of the  $d$  offset corrections. The quadratic sum of these systematic uncertainties is 0.40%. The beam position and size contribute a negligible systematic uncertainty. As a check of the procedure, the  $\Delta_{trim}$  value and the fit range in  $X$  are varied; the resulting variations in the fitted slope are consistent with those observed for Monte Carlo events and no additional systematic uncertainty is assumed. The total systematic uncertainty, including the contribution from Monte Carlo statistics, is 0.45%.

The statistical uncertainty on  $\tau_\tau$  is multiplied by 1.03 in order to take into account the small dependence of the trimming bias on  $\tau_\tau$ . The uncertainty on  $\bar{p}_\tau^0$  is negligible. The corrected  $a_1$  value corresponds to

$$\tau_\tau = 290.4 \pm 3.2 \text{ (stat)} \pm 1.3 \text{ (syst) fs.} \quad (4)$$

## 5 Decay length analysis

The DL method [3] is used to measure the mean lifetime of  $\tau$ 's decaying into three charged tracks. Three-prong hemispheres with  $\Sigma q = \pm 1$  are selected from the basic  $\tau^+\tau^-$  sample. The event sphericity axis is calculated from the reconstructed charged and neutral particles for each event containing a candidate decay. The three charged tracks are required to point within  $18^\circ$  of this axis. Neutral particles outside of this cone are discarded and the sphericity axis is recalculated. This procedure avoids the large error on the  $\tau$  direction (and consequent lifetime bias) which can occur in radiative events.

Decays with an identified electron are rejected to reduce contamination from photon

conversions. The decay vertex is fitted from the full three-dimensional track information provided by the detector. A candidate is retained only if the vertex fit gives a  $\chi^2$  CL greater than 3%. This cut rejects 38% of the candidates in data and 31% in Monte Carlo. Most of the rejected decays contain a VDET hit that is assigned to the wrong track.

For each candidate decay, the  $\tau$  flight distance is evaluated by means of a least-squares fit in which the  $\tau$  production and decay points are free to vary. The position and size of the luminous region and the position and uncertainty of the fitted decay vertex enter the fit; the  $\tau$  flight direction is constrained to be parallel, within an uncertainty of typically 15 mrad, to the event sphericity axis, calculated as described above. The  $\tau$  direction uncertainty is parametrized from simulated events as a function of the event sphericity; events with low sphericity tend to have low neutrino momenta and hence a smaller  $\tau$  direction uncertainty. The uncertainty on the fitted decay length is required to be less than 0.3 cm, whereas the typical decay length resolution is 0.06 cm. Decay candidates with a fitted decay length greater than 3 cm are discarded. This requirement removes two candidates whose reconstructed vertices coincide with the beam pipe (radius 5.4 cm). Figure 3 shows the decay length distribution for the remaining 10076 candidates.

The mean decay length  $\langle \ell \rangle$  is extracted from the decay length distribution by means of a maximum likelihood fit. The probability function is taken to be the convolution of a decreasing exponential with a Gaussian resolution function. The slope of the exponential is adjusted for each event according to the LEP energy, such that the fitted  $\langle \ell \rangle$  corresponds to  $\sqrt{s} = 91.25$  GeV. The decay length uncertainties, calculated event by event, are multiplied by a global scaling factor  $k$  which is free to vary in the fit. The fits to the data yield  $\langle \ell \rangle = 0.2174 \pm 0.0023$  cm and  $k = 1.20 \pm 0.02$ .

The bias on the mean decay length, calculated from  $\tau^+\tau^-$  Monte Carlo events, is  $(-0.81 \pm 0.38)\%$ , where the uncertainty is from Monte Carlo statistics.

A Monte Carlo study shows that background events from  $Z \rightarrow q\bar{q}$  have a mean decay length consistent with zero and yield a bias of  $(-0.26 \pm 0.09)\%$ ; this uncertainty reflects the Monte Carlo statistics and a 25% systematic contribution. The contamination from one-prong  $\tau$  decays with converted photons is less than 0.01%.

The effects of pattern recognition errors are studied by varying the vertex  $\chi^2$  CL cut between 1% and 5%; a systematic uncertainty of 0.42% is assigned, based on the observed variations in the mean decay length in data and Monte Carlo. If the CL cut is placed below 1% a large increase in  $k$  is observed in data and Monte Carlo, indicating the presence of non-Gaussian tails in the decay length resolution.

The use of a double-Gaussian parametrization of the decay length resolution yields a negligible change ( $<0.05\%$ ) in the fitted mean decay length. The systematic uncertainty associated with the parametrization of the  $\tau$  direction uncertainty is negligible. The uncertainties on the detector alignment parameters correspond to a negligible error on  $\langle \ell \rangle$ . The beam position and size contribute a negligible systematic uncertainty.

The systematic biases and uncertainties are listed in Table 3. The total bias is calculated to be  $(-1.07 \pm 0.57)\%$ . A correction for this bias is applied to the fitted mean decay length. The mean momentum of selected  $\tau$ 's in Monte Carlo events at  $\sqrt{s} = 91.25$  GeV is 45.24 GeV/ $c$ ; this value is used to convert the mean decay length to a mean proper lifetime:

$$\tau_\tau = 287.9 \pm 3.1 \text{ (stat)} \pm 1.6 \text{ (syst)} \text{ fs.} \quad (5)$$

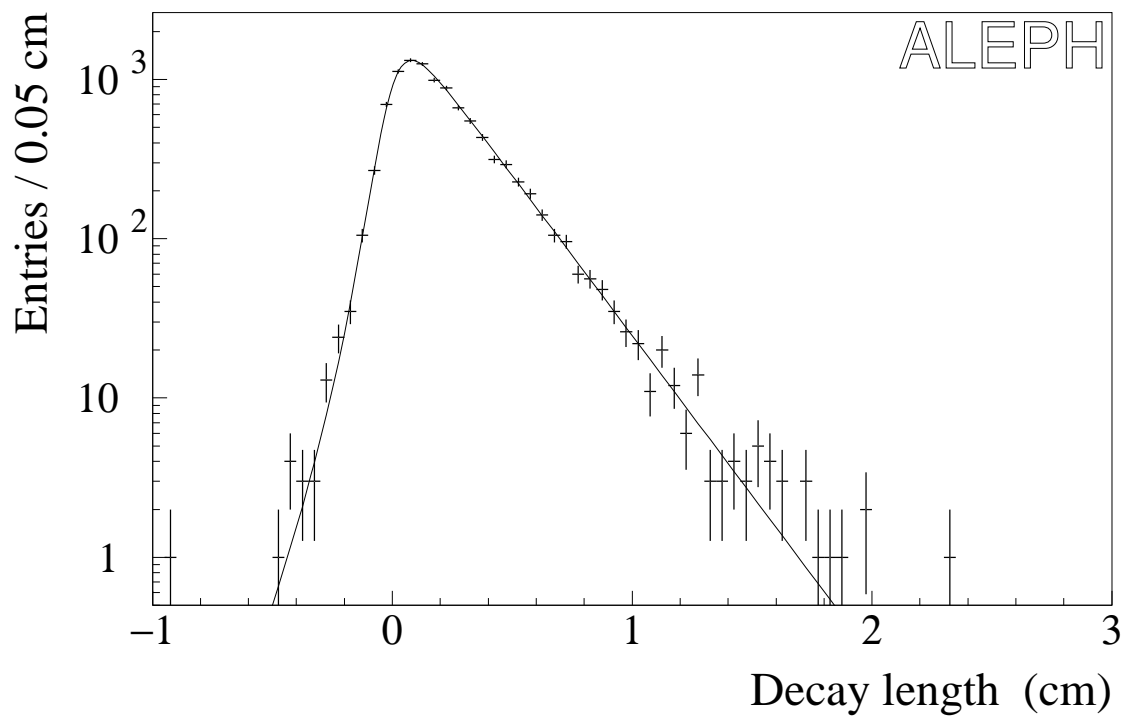


Figure 3: Decay length distribution for 1993 and 1994 data. The curve represents the sum of the functions obtained from separate fits to the two data samples.

Table 3: Systematic biases and uncertainties in the DL analysis.

Source	Bias and uncertainty (%)
$\tau^+\tau^-$ Monte Carlo bias	$-0.81 \pm 0.38$
Backgrounds	$-0.26 \pm 0.09$
Pattern recognition errors	$\pm 0.42$
Total bias and uncertainty	$-1.07 \pm 0.57$

## 6 Conclusions

The procedure of [17] is used to determine the optimum weights for averaging the measured lifetimes from the MIPS, IPD, and DL analyses. Correlations among the statistical and systematic errors are taken into account. The correlation coefficient of the MIPS and IPD statistical errors is calculated to be  $0.44 \pm 0.04$  in Monte Carlo events. The combined result for the 1993 and 1994 data is

$$\tau_\tau = 289.0 \pm 1.9 \text{ (stat)} \pm 1.3 \text{ (syst) fs}, \quad (6)$$

with  $\chi^2 = 0.29$  for 2 degrees of freedom (CL = 87%).

The three new results are combined with the previously published ALEPH measurements, including those obtained with the MIPS, IPD, DL, and other methods from data samples collected in 1989–1992 [1–3] and with the 3DIP method from the 1992–1994 data [4]. The statistical correlations involving 3DIP are detailed in [4]. The combined ALEPH result is

$$\tau_\tau = 290.1 \pm 1.5 \text{ (stat)} \pm 1.1 \text{ (syst) fs}, \quad (7)$$

with  $\chi^2 = 9.1$  for 15 degrees of freedom (CL = 87%). This result, the most precise measurement of the mean  $\tau$  lifetime, is consistent with other recent measurements [18].

The ALEPH measurements of the  $\tau$  lifetime and branching fractions may be used to test lepton universality. For  $B(\tau \rightarrow e\nu\bar{\nu}) = (17.79 \pm 0.12 \pm 0.06)\%$  [15],  $B(\tau \rightarrow \mu\nu\bar{\nu}) = (17.31 \pm 0.11 \pm 0.05)\%$  [15], and other quantities from [5], the ratios of the effective coupling constants [19] are

$$\frac{g_\tau}{g_\mu} = 1.0004 \pm 0.0032 \pm 0.0038 \pm 0.0005 \quad (8)$$

and

$$\frac{g_\tau}{g_e} = 1.0007 \pm 0.0032 \pm 0.0035 \pm 0.0005, \quad (9)$$

where the first uncertainty is from the  $\tau$  lifetime, the second is from the  $\tau$  leptonic branching fraction ( $B(\tau \rightarrow e\nu\bar{\nu})$  in Eq. 8 and  $B(\tau \rightarrow \mu\nu\bar{\nu})$  in Eq. 9), and the third is from the  $\tau$  mass. The measured ratios are consistent with the hypothesis of lepton universality.



# Acknowledgements

We wish to thank our colleagues in the CERN accelerator divisions for the successful operation of LEP. We are indebted to the engineers and technicians in all our institutions for their contribution to the excellent performance of ALEPH. Those of us from non-member countries thank CERN for its hospitality.

# References

- [1] ALEPH Collaboration, Phys. Lett. B **279** (1992) 411.
- [2] ALEPH Collaboration, Phys. Lett. B **297** (1992) 432.
- [3] ALEPH Collaboration, Z. Phys. C **70** (1996) 549.
- [4] ALEPH Collaboration, Z. Phys. C **74** (1997) 387.
- [5] R.M. Barnett et al. (Particle Data Group), Phys. Rev. D **54** (1996) 1.
- [6] ALEPH Collaboration, Nucl. Instrum. Methods A **294** (1990) 121.
- [7] B. Mours et al., Nucl. Instrum. Methods A **379** (1996) 101.
- [8] ALEPH Collaboration, Z. Phys. C **62** (1994) 539.
- [9] Computer program KORALZ, version 4.0, courtesy of S. Jadach, B.F.L. Ward, and Z. Wąs; S. Jadach and Z. Wąs, Comp. Phys. Commun. **36** (1985) 191; Monte Carlo Group in “Proceedings of the Workshop on Z Physics at LEP”, CERN Report 89-08 (1989) Vol. III; S. Jadach, B.F.L. Ward, and Z. Wąs, Comp. Phys. Commun. **79** (1994) 503.
- [10] Computer program UNIBAB, version 2.02; H. Anlauf et al., Comp. Phys. Commun. **79** (1994) 466.
- [11] Computer program HVFL, version 5; ALEPH Collaboration, Z. Phys. C **62** (1994) 179.
- [12] ALEPH Collaboration, Phys. Lett. B **313** (1993) 509, and references therein.
- [13] ALEPH Collaboration, Z. Phys. C **69** (1996) 183.
- [14] Computer program KORALB (modified version); S. Jadach and Z. Wąs, Comp. Phys. Commun. **64** (1991) 267.
- [15] ALEPH Collaboration, Z. Phys. C **70** (1996) 561.
- [16] ALEPH Collaboration, Z. Phys. C **70** (1996) 579.
- [17] L. Lyons, D. Gibaut, and P. Clifford, Nucl. Instrum. Methods A **270** (1988) 110.

- [18] SLD Collaboration, Phys. Rev. D **52** (1995) 4828; DELPHI Collaboration, Phys. Lett. B **365** (1996) 448; OPAL Collaboration, Phys. Lett. B **374** (1996) 341; CLEO Collaboration, Phys. Lett. B **388** (1996) 402; L3 Collaboration, Phys. Lett. B **389** (1996) 187.
- [19] W. Marciano and A. Sirlin, Phys. Rev. Lett. **61** (1988) 1815.